Noname manuscript No.
(will be inserted by the editor)

The influence of the stagnation zone on the fluid dynamics at the nozzle exit of a confined and submerged impinging jet

Nicholas Jeffers · Jason Stafford · Ciaran Conway · Jeff Punch · Edmond Walsh

Received: date / Accepted: date

Abstract Low profile impinging jets provide a means to achieve high heat transfer coefficients while occupying a small quantity of space. Consequently, they are found in many engineering applications such as electronics cooling, annealing of metals, food processing, and others. This paper investigates the influence of the stagnation zone fluid dynamics on the nozzle exit flow condition of a low profile, submerged and confined impinging water jet. The jet was geometrically constrained to a round, 16mm diameter, square-edged nozzle at a jet exit to target surface spacing (H/D) that varied between 0.25 $<$ H/D $<$ 8.75. The influence of turbulent flow regimes is the main focus of this paper, however laminar flow data is also presented between 1350 $<$ Re $<$ 17300. A custom measurement facility was designed and commissioned to utilise Particle-Image Velocimetry (PIV) in order to quantitatively measure the fluid dynamics both before and after the jet exits its nozzle. The velocity profiles are normalised with the mean velocity across the nozzle exit. The primary objective of this paper is to present accurate flow profiles across the nozzle exit of an impinging jet confined to a low H/D, with a view to guide the boundary conditions chosen for numerical simulations confined to similar constraints.The results revealed in this paper suggest that the fluid dynamics in the stagnation zone strongly influences the nozzle exit velocity profile at confinement heights between 0 $<$ H/D $<$ 1. This is of particular relevance with regards to the choice of inlet boundary conditions in numerical models, and it was found that it is necessary to model a jet tube length L/D $>$ 0.5

N. Jeffers and J. Stafford
Bell Labs, Thermal Management Research Group, Alcatel-Lucent, Dublin, Ireland
E-mail: nick.jeffers@alcatel-lucent.com

C. Conway and J. Punch
Connect, Stokes Institute, University of Limerick, Ireland

E. Walsh
Osney Thermo-Fluids Laboratory, University of Oxford, United Kingdom

– where D is the inner diameter of the jet – in order to minimise modelling uncertainty.

Keywords Impinging submerged and confined jets · Stagnation zone backpressure · Nozzle inlet velocity profile

1 Introduction

Impinging jets are applied to a wide range of engineering applications including the annealing of metals and plastics, turbine blade cooling, food processing and, more recently, electronics cooling. This paper focuses on the nozzle exit velocity profile of an impinging jet confined to a low nozzle-to-plate spacing (H/D). There have been a number of reviews identifying the significant parameters that impact the fluid dynamics of an impinging jet – Webb and Ma [1], Lienhard [2], Martin *et al* [3], Jambunathan *et al* [4], Polat *et al* [5], and Garimella and Rice [6]. These fundamental parameters include: Prandtl number (Pr), nozzle-to-plate spacing (H/D), Reynolds number (Re), nozzle diameter, nozzle cross-section geometry, nozzle length-to-diameter (L/D), flow confinement, and inlet turbulence level. Changing any one of these parameters can influence the fluid dynamics at the nozzle exit of the impinging jet. The aim of this paper is to present accurate nozzle exit flow profiles of an impinging jet confined to a low H/D to inform the boundary conditions selected in numerical simulations confined to similar constraints.

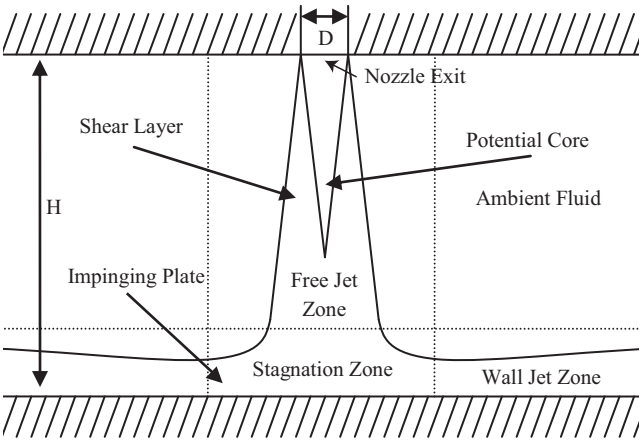

Fig. 1 Impinging jet schematic illustrating the free jet zone, the stagnation zone, and the wall jet zone

The features of an impinging jet can be divided into three distinctly different zones: the free jet zone; the stagnation zone; and the wall jet zone, as shown in Fig 1.

- The free jet zone refers to the region where the jet is unaffected by the impingement surface [7]. The free jet zone comprises a potential core surrounded by a shear layer. Within the potential core of the jet, both the fluid velocity and turbulence intensity remain unaffected by the shear layer. The shear layer entrains the ambient fluid creating high levels of turbulence that, in turn, cause both the radial spread of the jet, and the core diameter to diminish. When the shear layer penetrates the centre-line of the potential core, its axial velocity begins to decrease and the turbulence intensity begins to increase. Increasing distance from the nozzle exit sees a further decrease in centre-line velocity, and an increase in turbulence.
- The stagnation zone is created when a jet impinges onto a target surface. Within the stagnation zone, the axial velocity of the jet decelerates and is deflected in the radial direction. This zone initiates at the onset of the deceleration of axial velocity, which is caused by the impingement on the target surface. Martin [3] and Gardon and Akfirat [8] showed that the jet development begins to be influenced by the target surface at approximately $H/D = 1.2$ above the impinging surface. Fitzgerald and Garimella [9] also showed that for $H/D < 1.5$, the centre-line velocity drops rapidly as a result of the stagnation zone of the impinging jet.
- The wall jet zone exists beyond the radial limits of the stagnation zone, where the jet develops radially across the target surface. While complex fluid dynamics occur in this region, as shown by Jeffers [10], it is beyond the focus of this paper, which is concerned with the fluid dynamics across the jet's nozzle exit.

The velocity profile across the nozzle exit is generally a predefined boundary condition in the majority of numerical simulations found in the literature. This technique is used to simplify the model in order to save on computational time, especially if the model includes complex impingement features and arrays of jets. For convenience, the majority of these simulations employ either a fully-developed or undeveloped flat nozzle exit velocity profile as an inlet boundary condition. The ultimate precision of any numerical simulation relies on the accuracy of these predefined boundary conditions. Hadziabaic and Hanjalic [11] compiled a Large Eddie Simulation (LES) to model the fluid dynamics and heat transfer from a round jet impinging on a flat plate held at $H/D = 2$. They also generated a separate LES simulation to produce a fully-developed turbulent pipe flow, from which they extracted the fluid dynamics at every time step to replicate the nozzle exit condition of a fully-developed turbulent impinging jet. Hattori and Nagano [12] also used a fully-developed turbulent pipe flow to define the flow condition at the nozzle exit. Their primary objective was to model an impinging jet using Direct Numerical Simulation (DNS) and examine the effects of H/D spacings between $0.5 < H/D < 2.0$. Behnia *et al* [13] also employed a fully-developed turbulent flow profile for their nozzle inlet condition and performed a numerical analysis to determine the effects of jet confinement coupled with the influence of H/D ratios between $0.25 < H/D < 2$. Satake and Kunugi [14] performed a DNS simulation for an impinging jet

confined to a H/D = 6. They assumed that the velocity profile at the nozzle exit was fully-developed and turbulent. Thielen *et al* [15] compiled numerical simulations using $k - \varepsilon$ and $v^2 f$ methods to model impinging jet arrays confined to a H/D = 4 and utilised an undeveloped flat velocity profile across the nozzle exit. There are three physical parameters which influence the velocity profile at the nozzle exit: nozzle diameter to jet tube length (L/D) aspect ratio; the nozzle shape, and the fluid dynamics associated with the stagnation zone when the jet is confined to low H/D ratios.

This paper considers the influence of the stagnation zone on the velocity profile at the nozzle exit for low H/D confinements is sparse. There is literature that supports the notion that the fluid dynamics of the impinging jet change as the H/D ratio is reduced, however, the data presented is very limited. Fitzgerald and Garimella [9] showed that for H/D $>$ 1.5, the centre-line velocity of the jet was unaffected by the impinging plate, however, for H/D $<$ 1.5, the centre-line velocity of the jet drops rapidly. These results agree with those found by Martin *et al* [3] and Gardon and Akfirat [8] who reported that the target surface begins to have an effect at 1.2D. This paper aims to perform an in depth analysis of the influence of the stagnation zone on the nozzle exit flow conditions. The results from this study are of particular relevance for contemporary numerical simulations, where the nozzle exit condition is usually a predefined boundary condition to save on computational time. A submerged and confined water jet was experimentally assessed for Reynolds numbers between 1350 $<$ Re $<$ 17300, and confinement heights between 0.25 $<$ H/D $<$ 8.75. The main focus of this paper is towards turbulent jet flow regime, however, laminar flow data is also presented. Particle-Image Velocimetry (PIV) was used to quantitatively measure the flow fields surrounding the nozzle exit. The results presented show that the fluid dynamics in the stagnation zone of an impinging jet affect the nozzle exit velocity profile for confinement heights between 0 $<$ H/D $<$ 1. It was shown that as the H/D ratio decreases from H/D = 1, the stagnation zone backpressure effect increases. Pressure measurements were obtained at various locations along the jet tube to assess the influence of the stagnation zone with decreasing H/D. To support what was found experimentally, numerical simulations of a turbulent jet impingement were also conducted using the Reynolds-Averaged Navier-Stokes (RANS) approach. These models were used to predict the flow features generated as a result of the stagnation zone backpressure phenomena. A parametric study, using this numerical approach, was also conducted. This was used to assess the influence of the initial boundary conditions, assumed at the nozzle exit, on the predicted velocity fields above the impingement surface. The resultant findings from this paper can be used for clearly defining, and therefore reducing uncertainty, in the nozzle boundary condition when simulating low H/D jet impingement scenarios (i.e. H/D $<$ 1).

2 Detailed Analyses

The objective of this study is to evaluate the effects of the stagnation zone fluid dynamics on the nozzle exit velocity profile of an impinging jet confined to low H/D ratios. In order to achieve this objective, a custom measurement facility was created for experimental assessments, and a numerical model was developed to replicate this test facility. The experimental facility was capable of performing PIV, which was used to generate time-averaged velocity magnitude plots. PIV was chosen as it is a non-invasive method of achieving instantaneous 2D velocity vector field measurements. From these plots, the flow fields surrounding the stagnation zone of the jet were established. The experimental apparatus was also capable of recording pressure measurements within the jet tube at different locations. The experimental results were validated against theoretical velocity profile predictions. The experimental apparatus, test procedure, numerical analysis and uncertainty analysis are presented in this section.

2.1 Experimentation

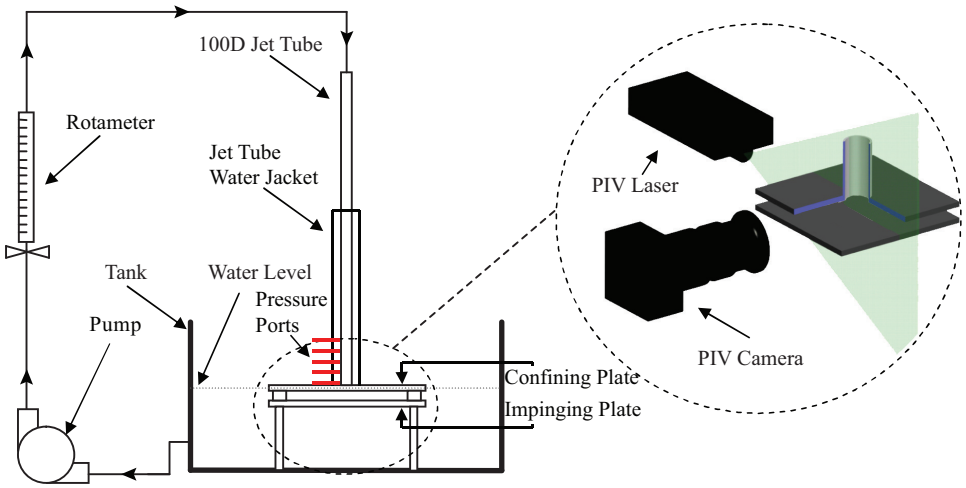

Fig. 2 PIV experimental apparatus

Velocity field measurements were taken using PIV on a confined and submerged water jet over a range of H/D ratios between $0.25 < H/D < 8.75$ to fully characterise the effect of this backpressure phenomenon surrounding the stagnation zone. Fig 2 shows the experimental apparatus used to visualise the fluid dynamics of a water jet. The jet in this facility exits a transparent straight round pipe with an inner diameter of 16mm, outer diameter 20mm,

and a length of 125 diameters (D). Kays *et al* [16] showed, for the range of Reynolds numbers (Re) tested in this paper, that fully-developed laminar and turbulent pipe flow occurs after 100D and 7D respectively. After the jet exits the tube, it impinges onto a flat plate (D=200mm). Thereafter the fluid is allowed to develop radially along the impinging plate, restricted only by a confining plate positioned at the nozzle exit. The water is then collected by a transparent reservoir tank positioned 200mm above the pump in order to obviate cavitation and to prevent air bubbles entering the system. Finally the water is returned to the pump, thus completing the flow circuit. A TSI PIV system was used to: visualise the flow field; extract velocity data from the jet flows; and to study the effect of stagnation zone fluid dynamics on the nozzle exit velocity profile.

The PIV parameters in this study were chosen to give the clearest velocity vector plots with the lowest uncertainties. This was achieved by matching the image capture rate and interrogation area to capture the dynamics of the flow. Generally, there are five parameters that can be varied to optimize the PIV results: laser sheet thickness; particle size and concentration; interrogation area size; distance between each pixel, which is affected by the image magnification and camera resolution; and the distance travelled by each particle, which is affected by the time interval between each laser pulse. Table 1 shows the parameters used in this experimentation for each of the flow visualisation experiments carried out.

Table 1 PIV parameters

PIV Parameters	H/D=0.25	H/D=0.37	H/D=0.62	H/D=1	H/D=8.75	Units
Length per pixel	10.71	14.46	14.56	17.46	17.24	[m]
Vector spacing	208	180	235	200	178	[m]
Interrogation size	40 X 40					[-]
Time between images	10 - 200					[s]
Laser sheet thickness	1.2					[mm]
Tracer particle size	8 - 12					[m]
Camera resolution	1600 X 1200					[pixel]

The experimentation apparatus was set up as shown in Fig 2. The laser was orientated to dissect the jet and the camera was orthogonally aligned and focused on the area of interest. The apparatus was filled with the working fluid to the water level shown in Fig 2. This level was chosen to reduce the effects of

ambient pressure on the flow structures formed. PIV tracer particles (silver-coated hollow glass spheres) were added until a sufficient concentration was met, as quantified by Reithmuller [17]. The tank was stirred until a homogeneous mixture of fluid to tracer particles was achieved within the system. The flow-rate in the system was adjusted by changing the voltage applied to the centrifugal pump. The flow rate recorded from the rotameter and the water properties – dictated by the temperature recorded in the tank – were used to calculate the Re number. One thousand image pairs were recorded for each of the Re tested. Both the fluid dynamics surrounding the stagnation zone and their influence along the jet tube were assessed over a range of Reynolds numbers between $1350 < \mathrm{Re} < 17300$ and for H/D ratios between $0.25 < \mathrm{H/D} < 8.75$. Generally, in jet analysis, Reynolds number is referenced to the jet's inner diameter (D) and the mean inlet velocity across the nozzle (V_m):

$$Re = \frac{\rho V_m D}{\mu} \tag{1}$$

Where ρ and μ are density and dynamic viscosity respectively. Velocity magnitude plots in this study are normalized to the mean inlet velocity of the jet (V_m) [17], [1].

Static pressure measurements were also evaluated near the nozzle exit. Measurements were taken at five different heights of 6mm, 8mm, 10mm, 54mm, and 104mm above the nozzle exit. At each height there were two static pressure measurements recorded using a manometer. Only two ports were open at any given time.

Experimental Uncertainty

The uncertainties in the primary measurements were minimized as follows: Flow rate uncertainty was minimised with the utilisation of two calibrated rotameters, which were capably of recording flow rates between the range of: 1.6 - 18 l/min with a maximum uncertainty of 12%; and 0.2 - 2 l/min with a maximum uncertainty of 15%; the uncertainty for the pressure measurements was minimised by recording two static pressure measurements with two separate manometers at each of the locations, as a result the pressure measurement uncertainty was 30Pa. In order to minimise the uncertainty within the PIV measurements, the following six rules developed by Keane and Adrian [18] and TSI [19] were strictly adhered to.

- One thousand particle image pairs, per interrogation area, were used in order to minimise the uncertainty in the statistical calculations for velocity magnitude.
- The interrogation area was chosen of sufficient size so that one vector reliably described the flow.
- In plane displacements greater than 25% of the interrogation size were avoided.
- In plane displacements less than two particle-image diameters were avoided.

– Out-of-plane displacements greater than 25% of the laser sheet thickness were avoided.
– The camera exposure and laser intensity was balanced and clearly showed the particles in the image.

Multiple image pairs were fully processed and the parameters varied until the above six rules were met and the system was aligned and focused.

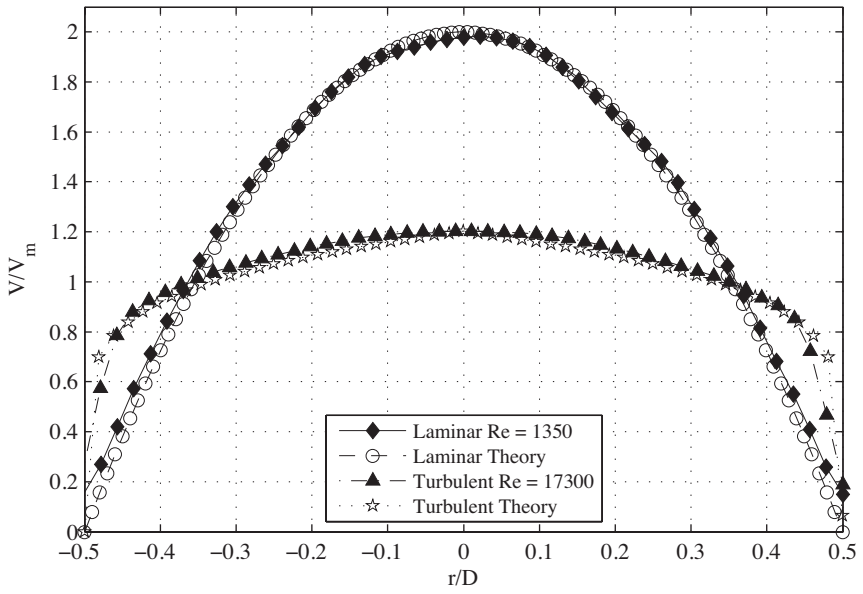

Fig. 3 Nozzle exit profiles extracted from the experimental results and compared to theoretical

In order to validate the experimental setup, the volumetric flow rate was calculated at the nozzle exit from the 1000 averaged PIV vector plots and compared to the values recorded by the rotameter. These results showed a maximum divergence of less than 8%. However, some of this variance is attributed to the uncertainty associated with the rotameter. Fig 3 plots the nozzle exit profiles for a jet confined to H/D = 8.75. The results are subsequently compared to the theoretical fully-developed nozzle exit profiles found in the literature [20]. Both the experimental and the theoretical profiles converge upon each other with a maximum deviation of only 2% between -0.45 < r/D < 0.45. This graph demonstrates the accuracy of the PIV results presented in this study having a maximum uncertainty of 8%.

2.2 Numerical Analysis

A numerical analysis was considered for a single turbulent flow case that was examined experimentally. This was the maximum Reynolds number (Re = 17300) and lowest nozzle to impingement plate distance H/D = 0.25, respectively. The primary aim of the numerical analysis was to examine the boundary condition parameters L/D and nozzle exit velocity profile on predictive accuracy. This analysis is used to provide recommendations for the numerical analysis of low H/D impinging jets.

A steady three-dimensional RANS approach was utilised for the numerical analysis. A solution to the governing equations of mass and momentum was achieved using the $k-\omega$ Shear Stress Transport (SST) model [21]. A second order scheme was implemented for discretisation and the analysis was performed using a double precision solver in ANSYS Fluent [22]. The standard and additional SST closure constants used for this approach remained as defined in Fluent [22]. This model was selected based on the findings of previous studies in the literature on jet impingement [23] [24]. Zuckerman and Lior [23] determined the most reliable numerical models that use the RANS approach for accurately predicting flow and heat transfer characteristics of impinging jets were the $k-\omega$ SST and v^2f models. A numerical model which replicated the experimental set-up described in Fig 2 was used to validate the numerical approach with the current experimental data as a benchmark. A velocity boundary condition was prescribed at the tube inlet. A pressure outlet boundary condition was defined at the exit of the computational domain, located 12.5D from the nozzle exit to reflect the experimental configuration in Fig 2.

Numerical Uncertainty

In all simulations, a velocity was defined at the inlet, an ambient pressure was defined at the outlet and a no-slip condition was set at the wall surfaces bounding the flow (impingement plate; confinement plate; inlet tube). The geometries were meshed using unstructured hexahedral cells and near wall refinement was achieved with $y^+ < 1$. A grid independence study was conducted to ensure results were insensitive to grid size (y^+ and global cell size). The final meshing parameters were selected to provide a trade-off between sufficient accuracy and limiting the demand on computational resources. The results of the mesh sensitivity study are listed in Table 2. Maximum local differences in the nozzle exit velocity profile for each grid over the largest grid size (mesh 5) are provided in Table 2. Five different grids were solved, spanning a ten-fold increase in node count. Using this information, mesh 3 was chosen as the most appropriate grid to solve the numerical simulations.

Table 2 Grid independence analysis on L/D=100 model

Mesh	Grid size (nodes)	Maximum local difference (%) Nozzle exit velocity profile
1	1.63×10^6	13.19
2	2.6×10^6	2.81
3	4.75×10^6	1.32
4	8.77×10^6	0.3
5	16.22×10^6	-

3 Results and Discussion

This section compares and discusses results found both experimentally and numerically to fully assess the influence that the stagnation zone has on the fluid dynamics at the nozzle exit of an impinging jet at low H/D ratios. Flow characteristics around the nozzle exit of a classical normally impinging, submerged and confined liquid jet are presented. The experimental apparatus and numerical setup discussed earlier were used to measure and predict full-field velocity magnitude plots. These plots are then used to illustrate the effect of the stagnation zone fluid mechanics on the jet's nozzle exit velocity profile.

A comparison between the numerically predicted and experimentally measured full-field velocity profiles at the nozzle exit is presented in Fig 4. Fig 4 (a) shows the experimentally measured PIV time-averaged velocity magnitude plot of a turbulent impinging jet confined to a H/D = 0.25 at a Re = 17300. The velocity magnitudes in every plot presented in this paper are normalised using the mean axial velocity across the nozzle exit (V_m). Fig 4 (b) shows the numerical prediction of the experimental configuration. The velocity magnitude numerical results are within 7% of those experimentally measured. This agreement is sufficient to validate the numerical model, as the difference is minor and within the same order of magnitude as the uncertainty in experimental measurement. Fig 4 (a) and (b) both show that the decelerating axial velocity in the stagnation zone influences the nozzle exit velocity profile. This deceleration in axial velocity is caused by the backpressure from the jet's impingement. This stagnation zone backpressure effect also influences the velocity profiles in the tube itself. Fig 4 (a) and (b) both show a steady decrease in velocity along the centre-line of the jet as it approaches the impingement surface. This decrease in centre-line velocity results in an increase in velocity around the periphery of the jet to conserve mass flow $(\rho V_m \pi D^2)/4$. As a result, the velocity profile at the nozzle exit has a lower velocity at the center than it does towards the periphery. This nozzle exit velocity profile is unique for low H/D ratios and neither resembles fully-developed nor undeveloped exit flow profiles. It is evident from both Fig 4 (a) and (b) that a combination of both physical constraints and fluidic backpressure effects define the shape of the nozzle exit velocity profile.

Fig 5 illustrates the effect of different confinement heights on the nozzle exit velocity profiles of a turbulent submerged and confined impinging jet at Re =

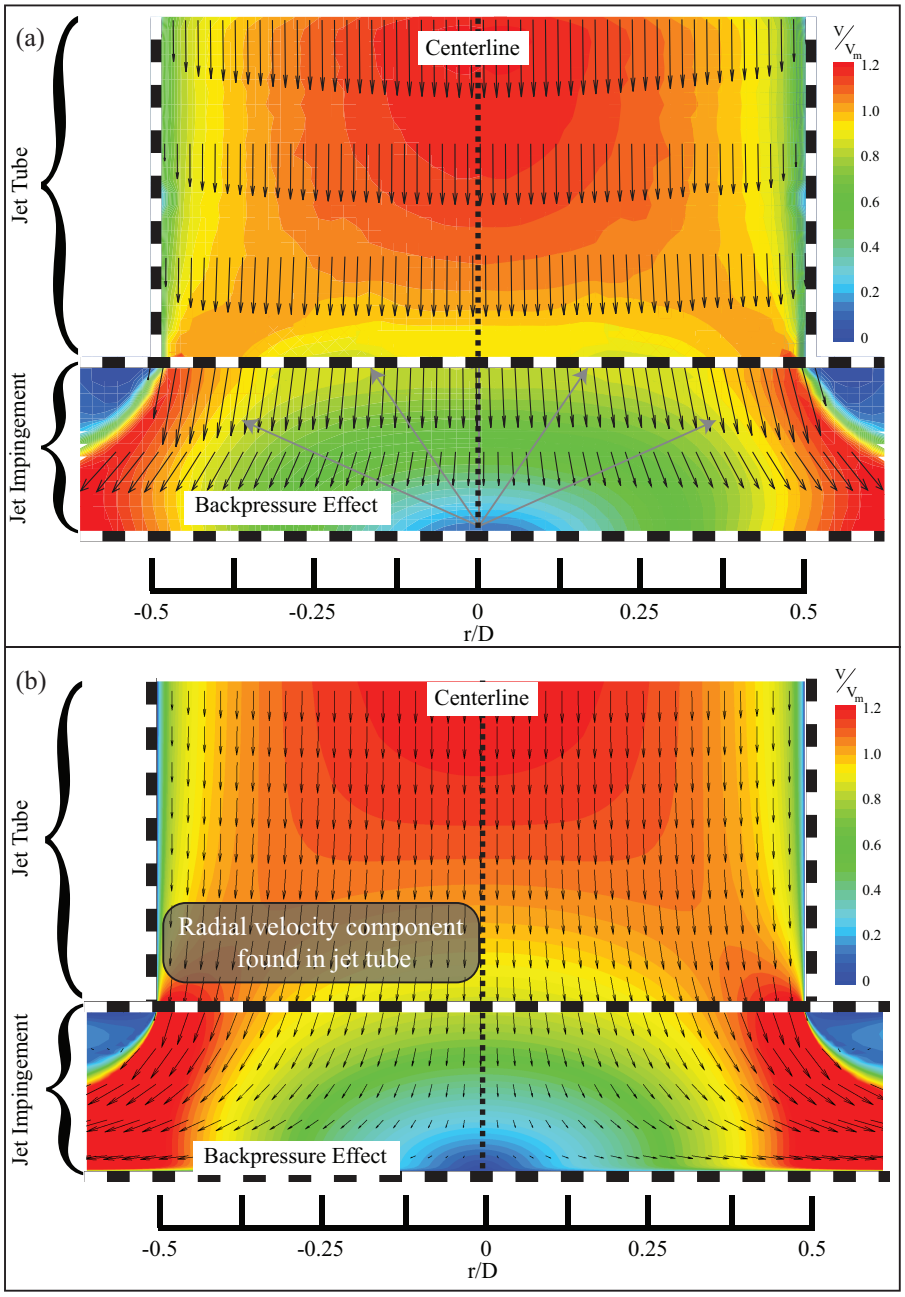

Fig. 4 Full-field velocity magnitude plots of a jet impingement, and its jet tube at H/D = 0.25 and Re = 17300 (a) Experimentally measured and (b) Numerically predicted

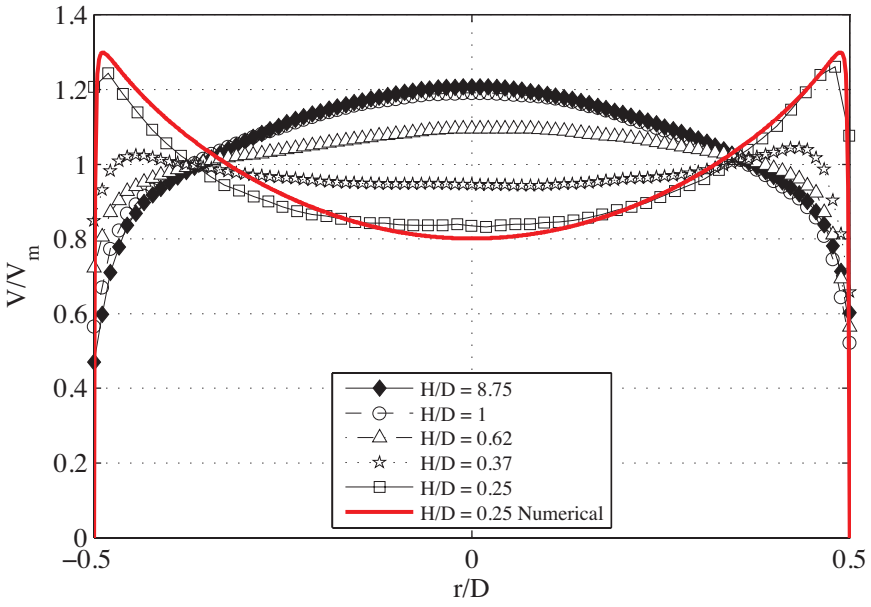

Fig. 5 Nozzle exit velocity profiles for a turbulent jet exiting at Re = 17300 showing the effect of different H/D confinement ratios

17300. As the confinement height is reduced from H/D = 1, the jet's centre-line velocity decreases while the velocity at the edge of the nozzle increases, as shown in Fig 5. As a result, the profile across the nozzle confined to a H/D = 0.25 has a peak velocity at the edge which decays to a trough at the centre-line of the jet, r/D = 0. The centre-line velocity (r/D = 0) is approximately 35% lower than the peak velocity for a nozzle confined to a H/D = 0.25. The fluidic mechanism responsible for the shape of the nozzle exit profile is the backpressure caused by the impingement in the stagnation zone. This backpressure region partially impedes the jet's centre-line flow, which results in an increase in velocity at the edge of the nozzle exit, as shown in Fig 5. For confinements H/D < 1, the profile resembles neither a fully developed nor developing nozzle flow, therefore to use either of these profiles as an initial boundary condition at the nozzle exit in a numerical model would result in errors.

Fig 6 illustrates the influence of Reynolds number on the velocity profiles across the nozzle exit for a confinement at H/D = 0.25. The profiles between 3400 < Re < 17300 conform together relatively well, with a maximum divergence across the nozzle exit of ∼11%. This shows that the normalised velocity profile between 3400 < Re < 17300 is largely independent of Reynolds number. The absent experimental results also show that for different H/D spacing, the normalised turbulent velocity profiles are independent of Re number. How-

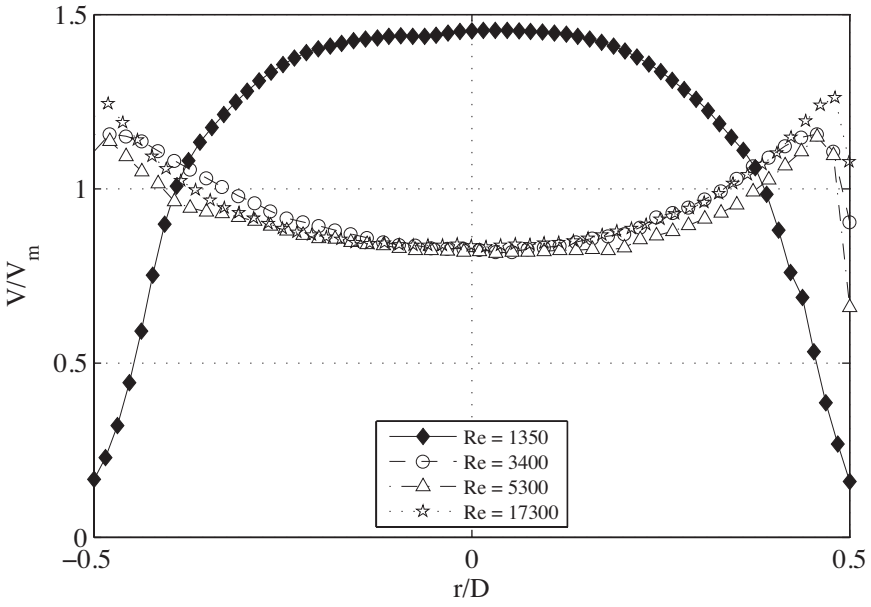

Fig. 6 Influence of Reynolds number on the jet inlet velocity profile for a confinement of H/D = 0.25

ever, the velocity at Re = 1350 exhibits a different profile as it is within the laminar regime. As a result, it is assumed that the only effect that a change in Reynolds number has on the normalised nozzle exit velocity profile is when the flow condition changes from laminar to turbulent regimes. As the nozzle exit velocity profiles are relatively insensitive to changes in Reynolds number, the numerical parametric study on the influence of nozzle boundary condition was conducted for a fixed Re = 17300 and also the lowest confinement height H/D = 0.25. Fig 5 plots the nozzle exit profiles with these constraints for both experimental and numerical results. They conform to within 4% of each other, thus further validating this numerical model.

Fig 7 shows the numerically predicted velocity magnitude plots for a range of initial boundary conditions. In order to save on computational time, simplified impinging jet models are used with predefined nozzle exit profiles. For low H/D confinements, this study shows that in reality the nozzle exit velocity profile is different to the conventional used fully developed or developing boundary conditions found in the literature [12] [13] [14] [15]. It is therefore important to examine the influence that an incorrectly defined nozzle exit boundary condition has on the surrounding fluid dynamics. Fig 7 (a) shows a numerically predicted stagnation zone that results from a predefined flat or developing velocity profile set 100D from the nozzle exit. This model was computationally demanding as the velocity profile within the entire 100D jet tube

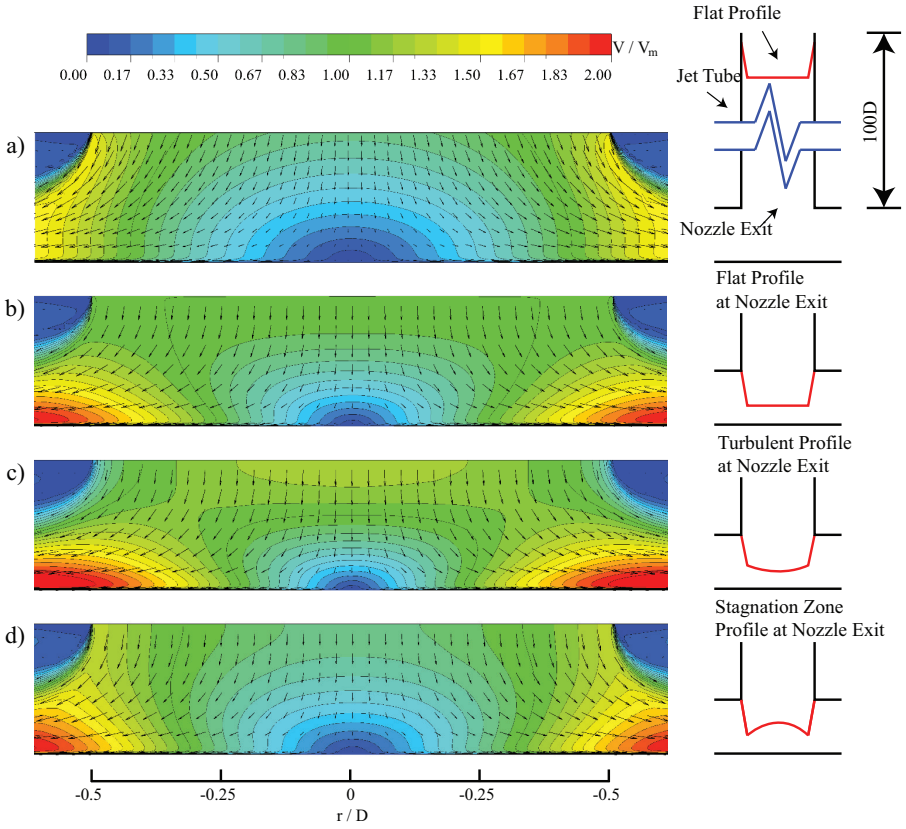

Fig. 7 Numerical prediction illustrating the velocity magnitude plots within the stagnation zone for an impinging jet at Re = 17300 and H/D = 0.25; the predefined velocity profile boundary conditions are, a) flat velocity profile set 100D from nozzle exit, b) flat profile at the nozzle exit, c) theoretical turbulent profile set at the nozzle exit, and d) a stagnation zone profile set at the nozzle exit

was solved. While the tube length is conservative considering development in turbulent pipe flow [16,25], it reflects the experimental arrangement in Fig 2. This result compares well with the experimental results found in Fig 4(a). The influence of inputting a predefined velocity condition at the nozzle exit is shown in Fig 7 for (b) flat developing profile, (c) theoretical turbulent profile and (d) axial nozzle exit profile extracted from Fig 7 (a). These boundary conditions result in different velocity magnitudes and fluid dynamics within the stagnation zone of an impinging jet when compared to both the experimental and numerical results, shown in Fig 4 (a) and Fig 7 (a) respectively. In particular, increased velocity gradients are evident at the impingement surface as the jet's flow is forced from an axial to radial direction. Fig 7 (d) shows the resultant plot from an axial stagnation zone input profile. Although this plot resembles the actual profiles better than Fig 7 (b) and (c), it is still er-

roneous. This is because the stagnation zone affects the fluid dynamics in the jet tube itself. Fig 4 (b) shows a radial velocity component in the jet tube that is not accounted for with this predefined plot. These incorrectly defined boundary conditions will also affect wall flux statistics such as heat and mass transfer at the impingement surface, especially if augmentations are made to the impingement surface in order to enhance heat transfer.

Fig 8 presents the nozzle exit velocity profiles that result from predefined velocity boundary condition profiles set at different heights (L/D) from its nozzle exit. Two initial velocity profiles are assessed: a uniform initial flow profile, Fig 8 (a); and a turbulent initial flow profile, Fig 8 (b). Using a uniform profile boundary condition, a jet tube with L/D $>$ 12 would need to be defined to produce a nozzle exit profile within 5% of the validated L/D=100 prediction. This is because the flow is still developing for L/D $<$ 12. For example, if a uniform velocity boundary condition is set at L/D = 1, the resultant centre line velocity profile at the nozzle exit (r/D = 0) is under predicted by ∼17% and the near wall velocity (r/D = 0.5) is over predicted by ∼15%. Kays *et al* [16] showed that in pipe flow, a fully developed turbulent condition is met after L/D = 7 and Bejan [25] suggested a similar entrance length scale, L/D ∼ 10. The discrepancy between their findings and what is presented here is caused by the stagnation zone backpressure effectively increasing the jet tube length (L/D) necessary for a fully developed profile to exist. Fig 8 (b) shows the influence of an initial turbulent flow profile set at different heights (L/D) on the nozzle exit profile. Again, if the desired nozzle exit profile were to be within 5% of the validated prediction (L/D = 100), a jet tube with a length L/D $>$ 0.5 would also need to be modelled. This decrease in required jet tube length (L/D) is expected, as the approaching flow no longer needs the additional development length required when imposing a uniform velocity boundary condition. Fig 8 (b) also highlights significant differences when using L/D $<$ 0.5. For L/D = 0.25, the centreline velocity is over predicted by ∼19%. In this configuration, the stagnation zone backpressure is not captured sufficiently, and a falsely high centreline velocity is imposed. From these results it shows that if the model is to truly represent (within 5%) a fully developed turbulent nozzle exit profile at low H/D, two actions are required: firstly, a jet tube length L/D $>$ 0.5 is needed; and secondly, a theoretically turbulent velocity boundary condition is required at the inlet of this jet tube. Fig 8 (b) also shows that for L/D $>$ 1 the jet tube length (L/D) has little influence over the flow profile of the impinging turbulent jet.

The impact of inlet boundary condition on the nozzle exit velocity profile has been demonstrated. Variations in nozzle exit velocity can also affect predictions of transport phenomena at the impingement surface. In the impingement zone, directly beneath the nozzle exit (-0.5 $<$ r/D $<$ 0.5), the local wall shear stress τ_w varies by up to + 30 % when using L/D = 1 and a uniform initial flow profile compared to the experimentally validated solution (L/D = 100). Considering Reynolds analogy as an estimate, St $\sim C_f/2$, predictions of local heat transfer coefficient in this impingement zone can vary by a similar magnitude. Although this simple analogy is limited, based on the current flow

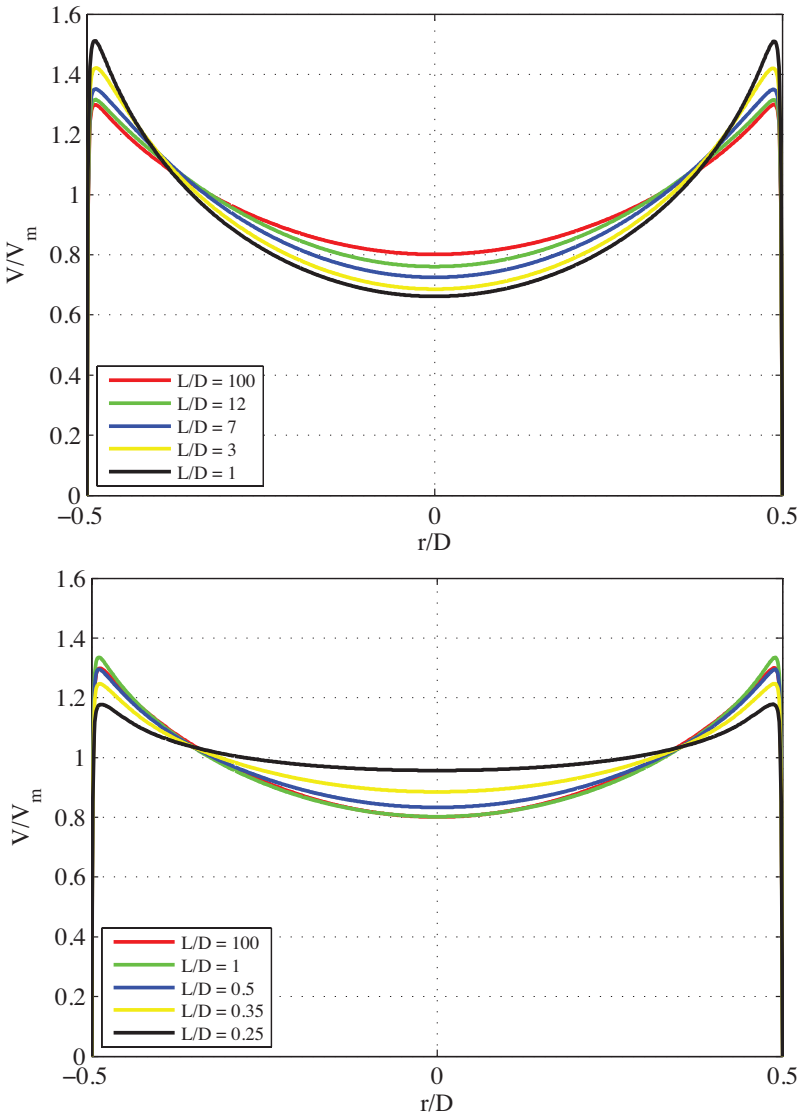

Fig. 8 Resultant nozzle exit velocity profiles for predefined boundary condition velocity profiles set between $0.25 < L/D < 100$ using (a) a uniform profile and (b) a fully developed turbulent flow profile

configuration and Prandtl number, it demonstrates the potential misrepresentation of heat transport through incorrect definition of boundary conditions at low H/D.

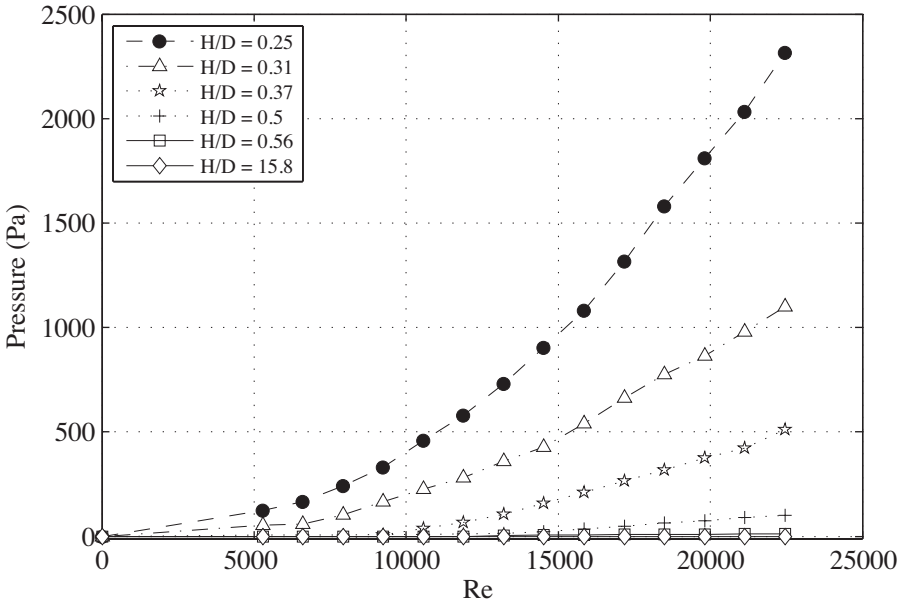

Fig. 9 Pressure results from static ports located 6mm before the nozzle exit for jet confinements between 0.25<H/D<15.8

Fig 9 shows the pressure results from a static port located 6 mm before the nozzle exit for different H/D jet confinements. There is almost no change in pressure as the H/D confinement is reduced to H/D = 0.5. However, as H/D is further reduced, the influence of the stagnation zone becomes prominent and the local pressure begins to increase rapidly. Pressure measurements were also recorded at five different locations above the nozzle exit (6mm, 8mm, 10mm, 54mm, and 104mm) and showed a maximum deviation of 14%.

The results found in this paper are of vital importance regarding the accurate modelling of impinging jets confined to low H/D ratios. It is self evident that if the initial boundary conditions of numerical models are not defined correctly, it propagates into predictive uncertainty regardless of the model that is being implemented. Similarly, the results of this parametric study can be used to provide useful estimates of numerical uncertainty due to boundary condition assumptions in turbulent impinging jet studies. It is recommended that a theoretical turbulent velocity profile is inputted at the inlet of a jet tube with a length L/D > 0.5 when simulating a fully developed turbulent jet at low H/D spacing. This finding is important with regards to complex models addressing impingement surface augmentations or arrays of jets or both. Numerical analyses such as DNS will also indirectly benefit from this work, as there may not be a need to model the entire jet tube, which is computationally demanding.

4 Conclusions

This paper describes the nozzle exit velocity profiles for a classical normally impinging submerged and confined liquid jet. The velocity profiles used as boundary conditions within the computational fluid dynamic literature do not account properly for the stagnation zone backpressure effect. The objective of this paper is to present experimental and numerical results to illustrate the effect that the stagnation zone backpressure has on the nozzle exit velocity profile for low H/D ratios. The following conclusions are inferred:

- Within the stagnation zone of an impinging jet, the fluid's velocity is influenced by the target surface causing a deceleration in axial velocity constituting an impingement. The backpressure as a result of this impingement affects the nozzle exit velocity profile for $H/D < 1$.
- As the H/D ratio is reduced, the stagnation zone backpressure effect increases. For a turbulent jet issuing at $Re = 17300$ and confined to a $H/D = 0.25$, the velocity profile across the nozzle exit shows a peak towards the edge followed by a trough with a 35% drop in velocity towards the centre. The laminar jet's nozzle velocity profile is effectively compressed as H/D is reduced, and shows a 30% reduction in centre-line velocity.
- Laminar and turbulent jets exhibit different nozzle exit velocity distributions even at low H/D, although their shape is still strongly influenced by the stagnation zone backpressure.
- The static pressure readings near the nozzle exit show that, pressure the influence of the stagnation zone backpressure is only significant for $H/D < 0.5$.
- The selection of a suitable inlet boundary condition is an important factor for capturing the stagnation zone backpressure and validating the suitability of numerical models with experimental data. The numerical results show that if the model is to represent a fully developed turbulent nozzle exit profile within a 5% accuracy, the following two initial boundary conditions must be adhered to: i) a jet tube length $L/D > 0.5$, and ii) a theoretically turbulent velocity boundary condition at the inlet.

This paper shows that the nozzle exit velocity profile is heavily influenced by the stagnation zone backpressure effect for low H/D constraints. The results from this study can be used to generate nozzle exit velocity profiles with greater accuracy for numerical simulations confined to similar conditions.

5 Compliance with Ethical Standards

Conflict of Interest: The authors declare that they have no conflict of interest.

Acknowledgements Bell Labs would like to thank the Industrial Development Agency (IDA) Ireland for their continued support. Connect would like to thank Science Foundation Ireland for their financial support.

References

1. B. Webb and C. Ma, "Single-phase liquid jet impingement heat transfer," *Advances in Heat Transfer*, vol. 26, pp. 105–217, 1995.
2. J. Lienhard, "Liquid jet impingement," *Annual Review of Heat Transfer*, vol. 6, pp. 199–270, 1995.
3. H. Martin, P. James, J. Thomas, and F. Irvine, "Heat and mass transfer between impinging gas jetsand solid surfaces," *Advances in Heat Transfer*, vol. 13, pp. 1–60, 1977.
4. K. Jambunathan, E. Lai, M. Moss, and B. Button, "A review of heat transfer data for single circular jet impingement," *International Journal of Heat and Fluid Flow*, vol. 13, no. 2, pp. 106 – 115, 1992.
5. S. Polat, B. Huang, S. Mujumdar, and W. Douglas, "Numerical flow and heat transfer under impinging jets: a review," *Annual Review of Numerical Fluid Mechanics and Heat Transfer*, vol. 2, pp. 157–197, 1989.
6. S. V. Garimella and R. A. Rice, "Confined and submerged liquid jet impingement heat transfer," *Journal of Heat Transfer*, vol. 117, pp. 871–877, 11 1995.
7. M. D. Deshpande and R. N. Vaishnav, "Submerged laminar jet impingement on a plane," *Journal of Fluid Mechanics*, vol. 114, pp. 213–236, 1 1982.
8. R. Gardon and J. Akfirat, "The role of turbulence in determining the heat-transfer characteristics of impinging jets," *International Journal of Heat and Mass Transfer*, vol. 8, no. 10, pp. 1261 – 1272, 1965.
9. J. A. Fitzgerald and S. V. Garimella, "A study of the flow field of a confined and submerged impinging jet," *International Journal of Heat and Mass Transfer*, vol. 41, no. 8â9, pp. 1025 – 1034, 1998.
10. N. Jeffers, "On the heat transfer and fluid mechanics of a normally-impinging, submerged and confined liquid jet," *PhD Thesis from the University of Limerick, Ireland*, 2009.
11. M. Hadziabdic and K. Hanjalic, "Vortical structures and heat transfer in a round impinging jet," *Journal of Fluid Mechanics*, vol. 596, pp. 221–260, 1 2008.
12. H. Hattori and Y. Nagano, "Direct numerical simulation of turbulent heat transfer in plane impinging jet," *International Journal of Heat and Fluid Flow*, vol. 25, no. 5, pp. 749 – 758, 2004.
13. M. Behnia, S. Parneix, Y. Shabany, and P. Durbin, "Numerical study of turbulent heat transfer in confined and unconfined impinging jets," *International Journal of Heat and Fluid Flow*, vol. 20, no. 1, pp. 1 – 9, 1999.
14. S. Satake and T. Kunugi, "Direct numerical simulation of an impinging jet into parallel disks," *International Journal of Numerical Methods for Heat & Fluid Flow*, vol. 8, no. 7, pp. 768–780, 1998.
15. L. Thielen, K. Hanjalic, H. Jonker, and R. Manceau, "Predictions of flow and heat transfer in multiple impinging jets with an elliptic-blending second-moment closure," *International Journal of Heat and Mass Transfer*, vol. 48, no. 8, pp. 1583 – 1598, 2005.
16. W. Kays, M. Crawford, and B. Weigand, *Convective heat and mass transfer*. New York: McGraw and Hill, 2004.
17. M. Riethmuller, "Particle image velocimetry," *vonKarman Institute for Fluid Dynamics -Lecture Series*, 2003.
18. R. D. Keane and R. J. Adrian, "Optimization of particle image velocimeters, part 1, double pulsed systems," *Measurement Science and Technology*, vol. 1, no. 11, pp. 1202–1215, 1990.
19. TSI, "Particle image velocimetry (piv): Theory of operation."
20. R. Fox, A. McDonald, and P. Pritchard, *Introduction to fluid mechanics*, vol. 6. New Jersey: Wiley, 2004.
21. F. R. Menter, "Two-equation eddy-viscosity turbulence models for engineering applications," *AIAA Journal*, vol. 32, pp. 1598–1605, 2015/03/24 1994.
22. *ANSYS Fluent User's Guide*. Canonsburg, Pennsylvania: ANSYS Inc., 14 ed.
23. N. Zuckerman and N. Lior, "Radial slot jet impingement flow and heat transfer on a cylindrical target," *Journal of Thermophysics and Heat Transfer*, vol. 21, no. 3, 2007.
24. N. Zuckerman and N. Lior, "Jet impingement heat transfer: Physics, correlations, and numerical modeling," *Advances in Heat Transfer*, vol. 39, pp. 565–631, 2011.
25. A. Bejan, *Convection heat transfer. 3rd Ed. New Jersey:,*. New Jersey: Wiley, 3rd ed., 2004.